Generic Model Control for Lithium-Ion Batteries

Manan Pathak,[a,*] Suryanarayana Kolluri,[a,*] and Venkat R. Subramanian[a,b,,z]**

[a]*Department of Chemical Engineering, University of Washington, Seattle, Washington 98195, USA*
[b]*Pacific Northwest National Laboratory, Richland, Washington 99352, USA*

Battery Management Systems (BMS) are critical to safe and efficient operation of lithium-ion batteries and accurate prediction of the internal states. Smarter BMS that can estimate and implement optimal charging profiles in real-time are important for advancement of the Li-ion battery technology. Estimating optimal profiles using physics-based models is computationally expensive because of the non-linear and stiff nature of the model equations, involving the need for constrained nonlinear optimization. In this work, we present an alternative approach to control batteries called as Generic Model Control, or Reference System Synthesis. This work enables robust stabilization and control of battery models to set-point as an alternative approach, eliminating the need to perform optimization of nonlinear models. As compared to the generic model control approaches implemented by previous researchers, we implement the same concept using direct DAE numerical solvers. The results are presented for single input single objective problems, and for constrained problems for various battery models.

Manuscript submitted October 11, 2016; revised manuscript received February 16, 2017. Published March 14, 2017. This was Paper 208 presented at the San Diego, California, Meeting of the Society, May 29- June 2, 2016.

Lithium-ion batteries are used in a wide range of applications ranging from cell phones to electric vehicles (EVs) to electric grids. With the expected decline in the price of batteries over the next few years, the market for EVs and grids is growing rapidly. Long recharging times, capacity fade and thermal runaway are some of the main issues that need to be addressed in order to use batteries safely and efficiently for a longer time. This necessitates the use of smarter battery management systems that can derive optimal use strategies by exploiting the dynamics of the battery.

Battery models based on transport, physical, electrochemical and thermodynamics principles can be used to monitor the internal states of the battery and to obtain optimal control strategies. Such models are computationally expensive which limits their use in control applications in real-time. Various issues, such as the onset of dynamics of some internal states only during use of batteries at high charge/discharge rates, and several other states which are active only while charging or discharging, adds to the challenges of the observability of these physics-based electrochemical models. Hence, various approximated and reduced order models have been proposed in the past, to make the models strongly observable in local intervals.[1,2–5] These models are also highly non-linear in nature, which adds significant challenges to implement control strategies along with the above-mentioned issues. Past researchers have shown multivariable control techniques like Dynamic Matrix Control (DMC),[6] Internal Model Control (IMC),[7] and Model Predictive Heuristic Control (MPHC)[8] for a variety of systems. However, these models suffer from their reliability on the linear approximations of the experimentally obtained step-response data and do not directly consider the full nonlinear model explicitly.

Several researchers have been working to design optimal charging profiles for batteries by implementing a wide range of control strategies. Methekar et al.[9] derived optimal charging profiles for maximizing the energy using the Control Vector Parameterization (CVP) approach. Rahimian et al.[10] calculated the charging current to minimize the capacity fade vs. cycle number using a single particle model (SPM). Perez et al.[11] obtained optimal charging profiles for batteries with constraints on temperature as well as concentration of lithium in solid and electrolyte phase. Suthar et al.[12] proposed optimal charging profiles for minimizing the intercalation induced stresses inside particle using simultaneous discretization approach. Hoke et al.[13] proposed a method to minimize the cost of battery charging in markets with variable electricity costs after accounting for battery degradation. However, all of these methods require nonlinear and robust optimization approaches.

In this article, we present an alternative approach to control batteries, applying the method of Generic Model Control (GMC),[14] also known as Reference System Synthesis.[15] This approach is based on a set-point strategy for the measured (state) variable. GMC has previously been implemented on various applications such as multistage flash desalination,[16] distillation column control,[17–19] control of nutrients – removing activated sludge systems,[20] armature current control of DC motor,[21] etc. In this article, we apply the GMC technique to physics-based battery models. Lee and Sullivan[14] originally proposed the GMC algorithm for ordinary differential equations (ODEs) and for problems in which the measured variable is not explicitly dependent on the manipulated variable. Here, we extend the GMC technique to differential algebraic equations (DAEs) with set points for algebraic variables, and for problems in which the output is directly dependent on control, for applying it to battery models. Application of GMC requires robust DAE solvers. By combining GMC approach with robust DAE solvers, we show the ability to reformulate some of the common control and optimization problems for batteries as direct simulation problems. By rewriting charging and optimization objective as set-point control problems, we derive control profiles using the GMC approach. While the theoretical internal stability for the GMC approach is yet to be proven unlike nonlinear model predictive control approaches,[22] in our experience, the GMC approach is computationally competitive as it avoids the need for optimization for unconstrained problems, and for problems with bounds on the manipulated variable. The gain in CPU time is obtained only if efficient and robust DAE solvers are used.

In subsequent sections, we discuss the theory behind the GMC framework, followed by case studies for applying GMC control formulation for a thin film nickel hydroxide electrode, a single particle model, along with discussing various objectives for a physics-based Li-ion battery model. For the physics-based Li-ion battery model, the first case demonstrates the problem formulation and implementation for obtaining a current profile for a set-point given on the charge stored in the battery. The second case considers a set-point of 4.2 V for voltage of the cell, without any bounds on the applied current, followed by current containing bounds.

*Electrochemical Society Student Member.
**Electrochemical Society Member.
[z]E-mail: vsubram@uw.edu

Generic Model Control

The generic model control (GMC) strategy is based on finding values for the manipulated variable that forces the controlled (measured) variable to reach its set-point in a non-linear process model. The desired set-point and its measured variable is compared to generate the error. The obtained error is used in GMC architecture to generate control input for the system (process dynamics) to direct the controlled variable toward the desired set-point.

The strategy for implementing generic model control is described as follows. Consider a dynamic process model given by a set of differential equations:

$$\frac{dx}{dt} = f(x, u, t) \quad [1]$$

where x is the vector of state variables of dimension n, u is the scalar process input (also called as manipulated variable) of dimension m, t is the time. The relation for output variables is given by:

$$Y = M(x, u) \quad [2]$$

where Y is a vector of output variables (measured variables) of dimension p.

To obtain control law from above Equations 1 and 2, a reference trajectory proposed by Lee and Sullivan[14] is given as,

$$\left(\frac{dY}{dt}\right) = K(Y^{set} - Y) + \frac{K}{\tau_i}\int_0^t \left(Y^{set} - Y\right) d\tau \quad [3]$$

where Y^{set} is the desired set-point, K and τ_i are the tuning parameters. The first term of the right hand side of Equation 3 is the rate of change of Y moving toward the desired set-point Y^{set}, and can be referred to as the *Proportional* term. The second term is added to minimize the offset between the actual value and the desired set-point, and can be referred to as the *Integral* term. Using Equation 3, a generic control law is obtained for GMC, which is given as,

$$\frac{dY}{dt} - K\left(Y^{set} - Y\right) - \frac{K}{\tau_i}\int_0^t \left(Y^{set} - Y\right) d\tau = 0 \quad [4]$$

The term $(\frac{dY}{dt})$ is the reference trajectory that can be obtained using Equations 1 and 2.

$$\left(\frac{dY}{dt}\right) = \frac{\partial M}{\partial x} f(x, u, t) + \frac{\partial M}{\partial u} \cdot \frac{du}{dt} \quad [5]$$

Combining Equations 4 and 5 gives the control law of GMC in terms of the process model and the reference trajectory.

$$\frac{\partial M}{\partial x} f(x, u, t) + \frac{\partial M}{\partial u}\frac{du}{dt} - K\left(Y^{set} - Y\right) - \frac{K}{\tau_i}\int_0^t \left(Y^{set} - Y\right) d\tau = 0 \quad [6]$$

Most physics-based battery models are given by partial differential equations (PDEs), which are converted to DAEs for simulation or optimization. Often times, the output or the measured variable is a direct function of the manipulated variable. Below, we discuss an approach to apply GMC for DAEs, including cases for which set point is given for an algebraic variable.

Consider an index-1DAE system governing two scalars y and z given by:

$$\frac{dy}{dt} = f(y, z, u) \quad [7]$$

$$g(y, z, u) = 0 \quad [8]$$

where, y is the differential variable, z is the algebraic variable and u is the manipulated variable. If the controlled (measured) variable is y, then Equations 4 and 6 can be used directly, as the derivative is explicitly available from the model equations. If the measured variable is z (for example potential as in the case of batteries), then the derivative $(\frac{dz}{dt})$ is not available directly from the model equations. The derivative $(\frac{dz}{dt})$ in such cases, can be obtained by differentiating Equation 8 with time to get:

$$\frac{dg}{dt} = \frac{\partial g}{\partial y}(y, z, u) \cdot f(y, z, u) + \frac{\partial g}{\partial z}(y, z, u) \cdot \frac{dz}{dt} + \frac{\partial g}{\partial u}(y, z, u) \cdot \frac{du}{dt} = 0 \quad [9]$$

GMC equation for this case is given by:

$$\left(\frac{dz}{dt}\right) = K(z^{set} - z) + \frac{K}{\tau_i}\int_0^t \left(z^{set} - z\right) d\tau \quad [10]$$

Equation 10 can now be substituted in Equation 9 to get:

$$\frac{dg}{dt} = \frac{\partial g}{\partial y}(y, z, u) \cdot f(y, z, u) + \frac{\partial g}{\partial z}(y, z, u) \cdot \left[K(z^{set} - z) + \frac{K}{\tau_i}\int_0^t \left(z^{set} - z\right) d\tau\right] + \frac{\partial g}{\partial u}(y, z, u) \cdot \frac{du}{dt} = 0 \quad [11]$$

In this case, Equation 7 governs the dynamics of the variable y, while variables z and u are governed by Equations 8 and 11 respectively. Even though a $\frac{du}{dt}$ term appears in 11, since the experimental value of z is known initially at time $t = 0$, the initial condition for u can be calculated using 8. The final form of the equations to be solved for obtaining the control profile is summarized in 12 as:

$$\left.\begin{aligned} &\frac{dy}{dt} = f(y, z, u) && \text{(a)}\\ &g(y, z, u) = 0 && \text{(b)}\\ &\frac{dg}{dt} = \frac{\partial g}{\partial y}(y, z, u) \cdot f(y, z, u) + \frac{\partial g}{\partial z}(y, z, u)\\ &\cdot\left[K(z^{set} - z) + \frac{K}{\tau_i}\int_0^t \left(z^{set} - z\right) d\tau\right] +\\ &\frac{\partial g}{\partial u}(y, z, u) \cdot \frac{du}{dt} = 0 && \text{(c)} \end{aligned}\right\} \quad [12]$$

Generic Model Control for Battery Models

In this section, we discuss the performance of generic model control strategy for different types of battery models.

Thin film nickel hydroxide electrode.—Consider the DAE model describing a galvanostatic charge of a thin-film nickel hydroxide electrode as described by Wu et al.[23] The model equations are given by:

$$\frac{dy_1}{dt} = \frac{j_1 \cdot W}{F\rho V} \quad [13]$$

$$j_1 + j_2 = I_{app} \quad [14]$$

$$\frac{dQ}{dt} = I_{app} \quad [15]$$

$$j_1 = i_{0,1}\left[2(1 - y_1)\exp\left(\frac{(\phi_1 - \phi_{01})F}{2RT}\right) - 2y_1\exp\left(-\frac{(\phi_1 - \phi_{01})F}{2RT}\right)\right] \quad [16]$$

$$j_2 = i_{0,2}\left[\exp\left(\frac{(\phi_1 - \phi_{02})F}{RT}\right) - \exp\left(-\frac{(\phi_1 - \phi_{02})F}{RT}\right)\right] \quad [17]$$

where y_1 is the mole fraction of nickel hydroxide, ϕ_1 represents the potential difference at the solid-liquid interface and Q is the total

Table I. Parameters of nickel hydroxide electrode.

Symbol	Parameter	Value	Units
F	Faraday constant	96,487	C/mol
R	Gas constant	8.314	J/(mol K)
T	Temperature	303.15	K
ϕ_{01}	Equilibrium potential	0.420	V
ϕ_{02}	Equilibrium potential	0.303	V
W	Mass of active material	92.7	g
V	Volume	1×10^{-5}	m^3
i_{01}	Exchange current density	1×10^{-4}	A/cm^3
i_{02}	Exchange current density	1×10^{-10}	A/cm^3
P	Density	3.4	g/cm^3

charge stored in the battery. I_{app} represents the applied current and is the manipulated variable for this model. The initial condition of the variables is $y_1(0) = 0.05$, $\phi_1(0) = 0.350236$, $Q(0) = 0$ and $I_{app}(0) = 1 \times 10^{-5}$. The parameters for this model are given in Table I.

For this model, three different objectives are studied as discussed below.

a) In the first objective, we solve the model for mole-fraction (y_1) to reach its desired set point (y_1^{set}). Even though this model is a DAE, the equation for the total derivative of the measured variable ($\frac{dy_1}{dt}$) is directly available from the model (Equation 13). This can be compared with Equation 2 to realize $Y = y_1$.

The GMC formulation for this case is given by:

$$\frac{dy_1}{dt} = \frac{j_1 \cdot W}{F\rho V} \quad [18]$$

$$\frac{dy_1}{dt} = K \cdot \left(y_1^{set} - y_1(t)\right) + \frac{K}{\tau_i} r(t) \quad [19]$$

where $r(t)$ represents the integral of the offset and is defined in Equation 20 as

$$\frac{dr}{dt} = \left(y_1^{set} - y_1(t)\right) \quad [20]$$

From Equations 18 and 19, the following relation can be derived:

$$\frac{j_1 W}{F\rho V} = K\left(y_1^{set} - y_1(t)\right) + \frac{K}{\tau_i} r(t) \quad [21]$$

Further, Equation 14 can be used to get:

$$\frac{\left(I_{app} - j_2\right) W}{F\rho V} = K\left(y_1^{set} - y_1(t)\right) + \frac{K}{\tau_i} r(t) \quad [22]$$

Using Equation 22, an explicit relation for I_{app} can be written as,

$$I_{app} = \frac{F\rho V}{W}\left(K\left(y_1^{set} - y_1(t)\right) + \frac{K}{\tau_i} r(t)\right) + j_2 \quad [23]$$

Equations 13–17 along with 23 are solved simultaneously to get the GMC control profile. The final set of equations (GMC model) to be solved for this case are summarized again in 24.

$$\left.\begin{aligned}
&\frac{dy_1}{dt} = \frac{j_1 \cdot W}{F\rho V} && \text{(a)}\\
&j_1 + j_2 = I_{app} && \text{(b)}\\
&\frac{dQ}{dt} = I_{app} && \text{(c)}\\
&\frac{dr}{dt} = \left(y_1^{set} - y_1(t)\right) && \text{(d)}\\
&I_{app} = \frac{F\rho V}{W}\left(K\left(y_1^{set} - y_1(t)\right) + \frac{K}{\tau_i} r(t)\right) + j_2 && \text{(e)}\\
&j_1 = i_{0,1}\left[2(1 - y_1)\exp\left(\frac{(\phi_1 - \phi_{01})F}{2RT}\right)\right.\\
&\qquad \left. -2y_1 \exp\left(-\frac{(\phi_1 - \phi_{01})F}{2RT}\right)\right] && \text{(f)}\\
&j_2 = i_{0,2}\left[\exp\left(\frac{(\phi_1 - \phi_{02})F}{RT}\right) - \exp\left(-\frac{(\phi_1 - \phi_{02})F}{RT}\right)\right] && \text{(g)}
\end{aligned}\right\} \quad [24]$$

It should be noted that the manipulated variable (I_{app}) is governed by Equation 24(e), whereas Equation 24(a), 24(b) and 24(c) govern y_1, ϕ_1 and Q respectively. The initial condition for $r(t)$ is assumed to be zero, the proportionality constant K is taken to be 0.02, and τ_i is assumed to be 3500. Figure 1a shows the profiles for mole fraction (y_1) for various set-points of $y_1^{set} = [0.5, 0.6, 0.7]$. Figure 1b shows the profiles of manipulated variable (I_{app})that directs mole fraction (y_1) to reach its desired set-point. An upper bound of 120 $\mu A/cm^2$ is used for this case. The strategy to implement bounded currents is explained in detail in the next example.

b) In the second case, the same DAE model is solved for total charged stored (Q) to reach its desired set point (Q^{set}). This case is similar to the case (a) discussed above. Equation 15 can be used to get the explicit derivative of the measured variable Q. Hence, for this case:

$$Y = Q$$

The GMC formulation is given by the following set of models,

$$\frac{dQ}{dt} = K\left(Q^{set} - Q(t)\right) + \frac{K}{\tau_i} r(t) \quad [25]$$

$$\frac{dr}{dt} = \left(Q^{set} - Q(t)\right) \quad [26]$$

From Equations 15 and 25, we can get:

$$I_{app}(t) = K\left(Q^{set} - Q(t)\right) + \frac{K \cdot r(t)}{\tau_i} \quad [27]$$

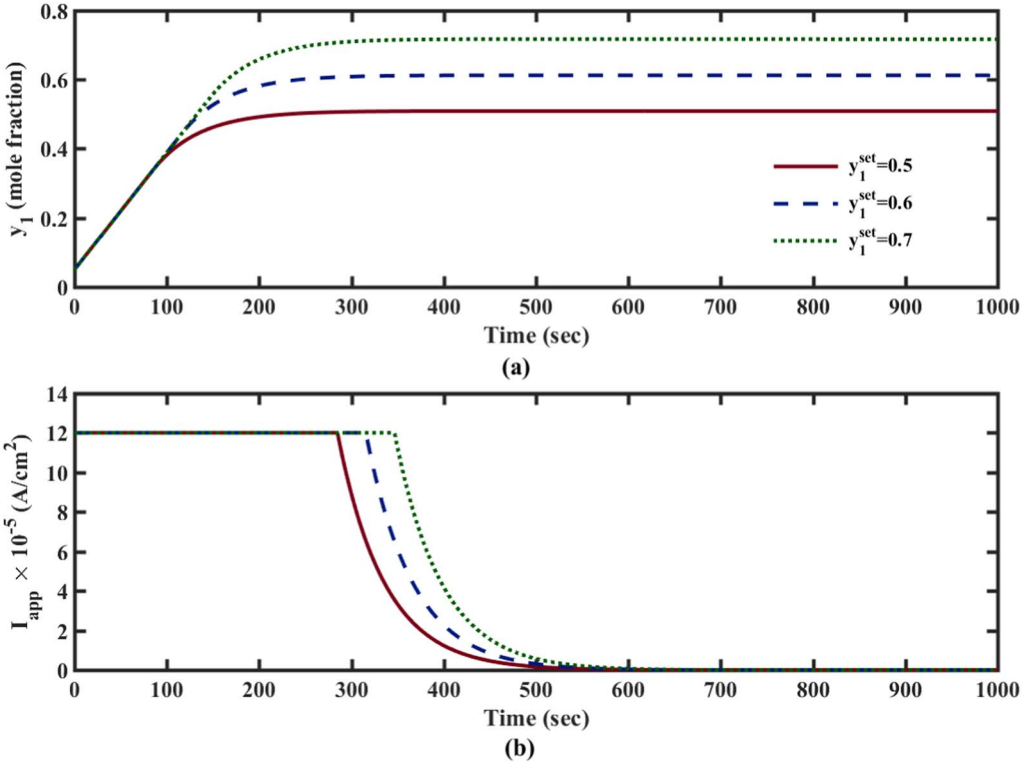

Figure 1. Profiles of (a) Mole fraction (y_1) and (b) Applied current (I_{app}) with time in the thin film nickel hydroxide electrode section (a).

If there are no bounds on current, the final set of equations to be solved for this case is given as follows:

$$\left.\begin{aligned}
&\frac{dy_1}{dt} = \frac{j_1 \cdot W}{F\rho V} && \text{(a)}\\
&j_1 + j_2 = I_{app} && \text{(b)}\\
&\frac{dQ}{dt} = I_{app} && \text{(c)}\\
&\frac{dr}{dt} = \left(Q^{set} - Q(t)\right) && \text{(d)}\\
&I_{app} = K\left(Q^{set} - Q(t)\right) + \frac{K}{\tau_i} r(t) && \text{(e)}\\
&j_1 = i_{0,1}\left[2(1-y_1)\exp\left(\frac{(\phi_1-\phi_{01})F}{2RT}\right) - 2y_1\exp\left(-\frac{(\phi_1-\phi_{01})F}{2RT}\right)\right] && \text{(f)}\\
&j_2 = i_{0,2}\left[\exp\left(\frac{(\phi_1-\phi_{02})F}{RT}\right) - \exp\left(-\frac{(\phi_1-\phi_{02})F}{RT}\right)\right] && \text{(g)}
\end{aligned}\right\} \quad [28]$$

The controller parameters for this case are K = 0.1 and $\tau_i = 20$, and the initial condition for $r(t)$ is taken to be zero. Different set points for charge stored are tried for this case.

In case if there are bounds on the applied current, it is bounded by applying upper and lower limits using relation given in Equation 27. Here, we assume a lower bound of zero, and an upper bound of 120 $\mu A/cm^2$. Such a case can be solved by introducing a dummy variable ($I_1(t)$), that represents the applied current in the GMC Equation 28(e), and the bounds are then applied on the current variable ($I_1(t)$) as shown in Equation 29.

$$I_{app}(t) = \min\left(12 \times 10^{-5}, \max\left(0, I_1(t)\right)\right) \quad [29]$$

For the bounded case, the final equations to be solved are summarized below.

$$\left.\begin{aligned}
&\frac{dy_1}{dt} = \frac{j_1 \cdot W}{F\rho V} && \text{(a)}\\
&j_1 + j_2 = I_{app} && \text{(b)}\\
&\frac{dQ}{dt} = I_{app} && \text{(c)}\\
&\frac{dr}{dt} = \left(Q^{set} - Q(t)\right) && \text{(d)}\\
&I_1 = K\left(Q^{set} - Q(t)\right) + \frac{K}{\tau_i} r(t) && \text{(e)}\\
&I_{app} = \min\left(12 \times 10^{-5}, \max\left(0, I_1\right)\right) && \text{(f)}\\
&j_1 = i_{0,1}\left[2(1-y_1)\exp\left(\frac{(\phi_1-\phi_{01})F}{2RT}\right) - 2y_1\exp\left(-\frac{(\phi_1-\phi_{01})F}{2RT}\right)\right] && \text{(g)}\\
&j_2 = i_{0,2}\left[\exp\left(\frac{(\phi_1-\phi_{02})F}{RT}\right) - \exp\left(-\frac{(\phi_1-\phi_{02})F}{RT}\right)\right] && \text{(h)}
\end{aligned}\right\} \quad [30]$$

Figure 2a shows the profiles for charge stored with time for various set points of $Q^{set} = [0.15, 0.2, 0.3]$ and Figure 2b shows the corresponding control profile current for different set points. It can be seen that the charge stored reaches its set point in all the cases.

c) In the third objective, the DAE model is solved for potential of the battery, ϕ_1 (which is an algebraic variable in this model) to

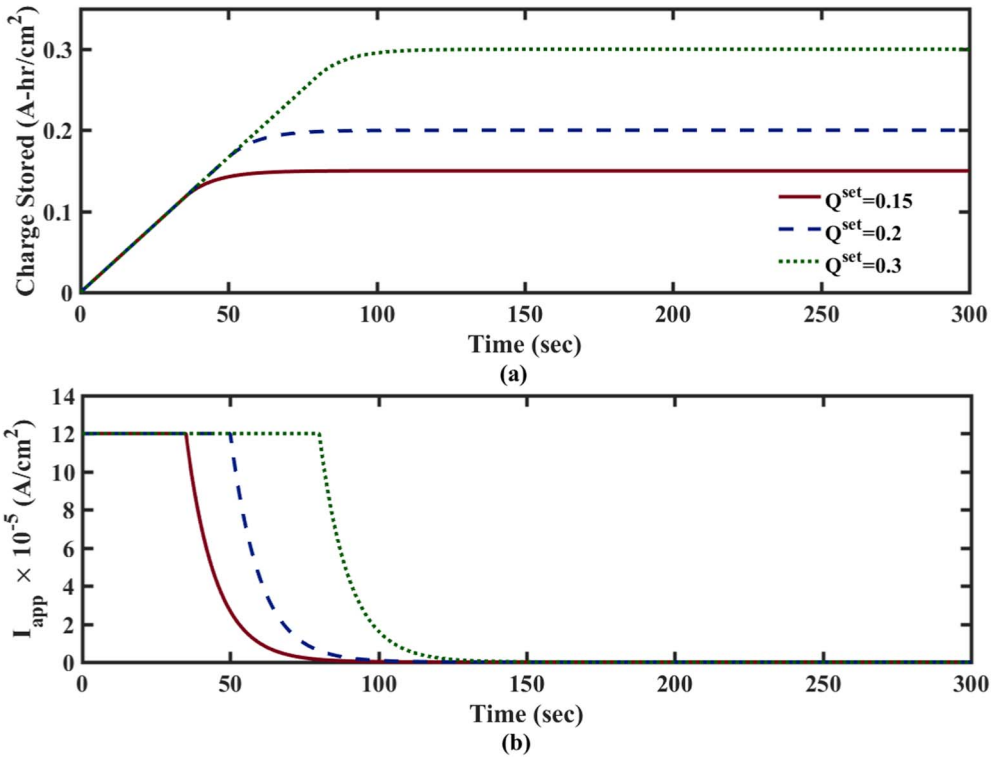

Figure 2. Profles of (a) Charge stored (Q) and (b) Applied current (I_{app}) with time in the thin film nickel hydroxide electrode section (b).

reach its desired set point ϕ_1^{set}. For this case,

$$Y = \phi_1$$

The full derivative ($\frac{d\phi_1}{dt}$) is not given by the model equations and $\frac{\partial g}{\partial u}(y, z, u)$ (in Equation 9) is not zero. The GMC formulation for this case is given by equations described earlier for the DAE model. Equations 16 and 17 can be substituted in 14 to get:

$$I_{app} = \left\{ \begin{array}{l} i_{0,1}\left[2\left(1-y_1\right)\exp\left(\dfrac{\left(\phi_1-\phi_{01}\right)F}{2RT}\right) \\ \quad -2y_1\exp\left(-\dfrac{\left(\phi_1-\phi_{01}\right)F}{2RT}\right)\right]+ \\ i_{0,2}\left[\exp\left(\dfrac{\left(\phi_1-\phi_{02}\right)F}{RT}\right)-\exp\left(-\dfrac{\left(\phi_1-\phi_{02}\right)F}{RT}\right)\right] \end{array} \right\} \quad [31]$$

Equation 31 can now be differentiated to get:

$$\frac{dI_{app}}{dt} = \left[\begin{array}{l} i_{0,1}\left[\begin{array}{l} 2\left(1-y_1\right)\exp\left(a_1\right)\cdot\frac{F}{2RT}\cdot\frac{d\phi_1}{dt}+2\exp\left(a_1\right)\left(-\frac{dy_1}{dt}\right) \\ -2y_1\exp\left(-a_1\right)\cdot\left(-\frac{F}{2RT}\right)\cdot\frac{d\phi_1}{dt}-2\exp\left(-a_1\right)\left(\frac{dy_1}{dt}\right) \end{array}\right]+ \\ i_{0,2}\left[\exp\left(a_2\right)\cdot\frac{F}{RT}\cdot\frac{d\phi_1}{dt}-\exp\left(-a_2\right)\cdot\left(-\frac{F}{RT}\right)\cdot\frac{d\phi_1}{dt}\right] \end{array}\right] \quad [32]$$

$$a_1 = \frac{\left(\phi_1-\phi_{01}\right)F}{2RT}, a_2 = \frac{\left(\phi_1-\phi_{02}\right)F}{2RT} \quad [33]$$

Equation 32 is rewritten for $\frac{d\phi_1}{dt}$ to get:

$$\frac{d\phi_1}{dt} = \frac{\frac{dI_{app}}{dt}+2i_{0,1}\exp\left(a_1\right)\left(\frac{dy_1}{dt}\right)+2i_{0,1}\exp\left(-a_1\right)\left(\frac{dy_1}{dt}\right)}{\left[\begin{array}{l} i_{0,1}\left[2\left(1-y_1\right)\exp\left(a_1\right)\cdot\frac{F}{2RT}-2y_1\exp\left(-a_1\right)\cdot\left(-\frac{F}{2RT}\right)\right]+ \\ i_{0,2}\left[\exp\left(a_2\right)\cdot\frac{F}{RT}-\exp\left(-a_2\right)\cdot\left(-\frac{F}{RT}\right)\right] \end{array}\right]} \quad [34]$$

Also, the equations for the GMC formulation is added as:

$$\frac{d\phi_1}{dt} = K\left(\phi_1^{set}-\phi_1\left(t\right)\right)+\frac{K\cdot r\left(t\right)}{\tau_i} \quad [35]$$

$$\frac{dr}{dt} = \left(\phi_1^{set}-\phi_1\left(t\right)\right) \quad [36]$$

From Equations 34 and 35, we can get:

$$\frac{\frac{dI_{app}}{dt}+2i_{0,1}\exp\left(a_1\right)\left(\frac{dy_1}{dt}\right)+2i_{0,1}\exp\left(-a_1\right)\left(\frac{dy_1}{dt}\right)}{\left[\begin{array}{l} i_{0,1}\left[\begin{array}{l} 2\left(1-y_1\right)\exp\left(a_1\right)\cdot\frac{F}{2RT}- \\ 2y_1\exp\left(-a_1\right)\cdot\left(-\frac{F}{2RT}\right) \end{array}\right]+ \\ i_{0,2}\left[\exp\left(a_2\right)\cdot\frac{F}{RT}-\exp\left(-a_2\right)\cdot\left(-\frac{F}{RT}\right)\right] \end{array}\right]} = K\left(\phi_1^{set}-\phi_1\left(t\right)\right)+\frac{K\cdot r\left(t\right)}{\tau_i} \quad [37]$$

Equations 13–17 are solved together along with Equations 36 – 37 to obtain the control profiles for this case. In order to implement bounds on the applied current, a similar dummy variable ($I_1(t)$), is added in the GMC equation. The final set of model equations solved for this

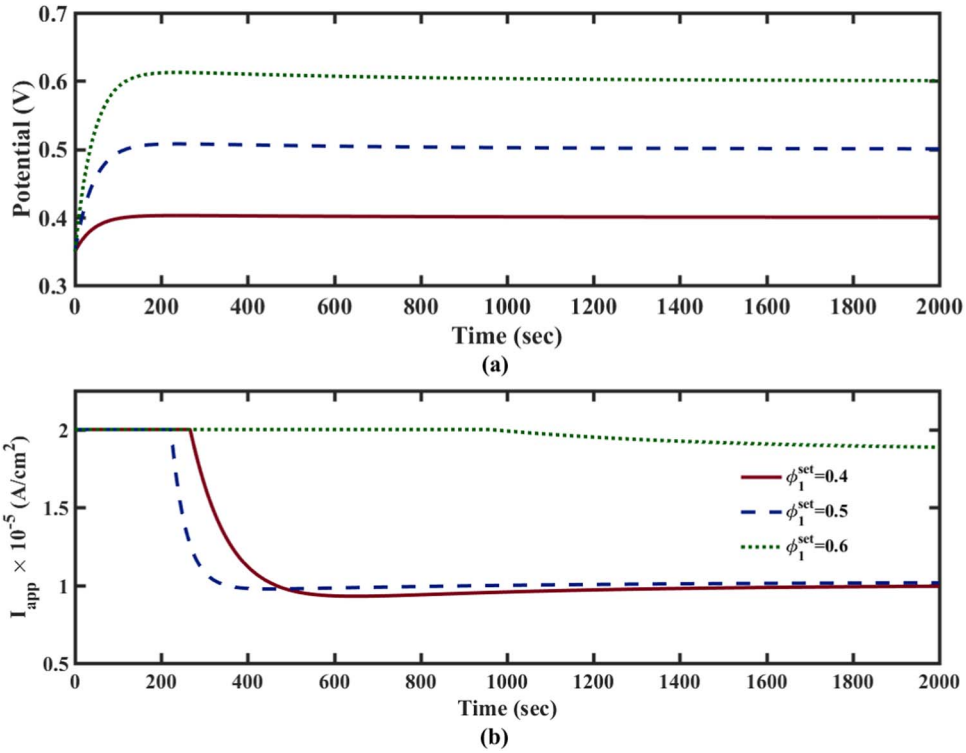

Figure 3. Profiles of (a) Potential(ϕ_1) and (b) Applied current (I_{app}) with time in the thin film nickel hydroxide electrode section (c).

case are summarized in Equation 38.

$$\left.\begin{aligned}
&\frac{dy_1}{dt} = \frac{j_1 \cdot W}{F\rho V} && \text{(a)}\\
&j_1 + j_2 = I_{app} && \text{(b)}\\
&\frac{dQ}{dt} = I_{app} && \text{(c)}\\
&\frac{dr}{dt} = \left(\phi_1^{set} - \phi_1(t)\right) && \text{(d)}\\
&\frac{\frac{dI_1}{dt} + 2i_{0,1}\exp(a_1)\left(\frac{dy_1}{dt}\right) + 2i_{0,1}\exp(-a_1)\left(\frac{dy_1}{dt}\right)}{\left[\begin{aligned} &i_{0,1}\left[2(1-y_1)\exp(a_1)\cdot\frac{F}{2RT} - 2y_1\exp(-a_1)\cdot\left(-\frac{F}{2RT}\right)\right] + \\ &i_{0,2}\left[\exp(a_2)\cdot\frac{F}{RT} - \exp(-a_2)\cdot\left(-\frac{F}{RT}\right)\right]\end{aligned}\right]} \\
&= K\left(\phi_1^{set} - \phi_1(t)\right) + \frac{K\cdot r(t)}{\tau_i} && \text{(e)}\\
&I_{app} = \min\left(2\times 10^{-5}, \max(0, I_1)\right) && \text{(f)}\\
&j_1 = i_{0,1}\left[2(1-y_1)\exp\left(\frac{(\phi_1-\phi_{01})F}{2RT}\right) - 2y_1\exp\left(-\frac{(\phi_1-\phi_{01})F}{2RT}\right)\right] && \text{(g)}\\
&j_2 = i_{0,2}\left[\exp\left(\frac{(\phi_1-\phi_{02})F}{RT}\right) - \exp\left(-\frac{(\phi_1-\phi_{02})F}{RT}\right)\right] && \text{(h)}
\end{aligned}\right\} \quad [38]$$

It can be noted that in this case, Equation 38b determines the variation of the measured variable with time, and Equations 38e and 38f govern the control profile. The controller parameters for this case are K = 0.0250 and $\tau_i = 15$. Figure 3 shows the results obtained for this case. Figures 3a and 3b show the potential and current profiles respectively obtained for different set points $\phi_1^{set} = [0.4, 0.5, 0.6]$.

Single particle model.—A single particle model[10] for an electrode is used to illustrate the concept for a model with multiple algebraic equations in the DAE system. Consider diffusion of a particle inside a spherical electrode. The model equations for this case are given by:

$$\frac{\partial c}{\partial t} = \frac{1}{r^2}\cdot\left(\frac{\partial}{\partial r}\left(r^2\frac{\partial c}{\partial r}\right)\right) \quad [39]$$

With the boundary conditions

$$\text{At } r = 0,\ \frac{\partial c}{\partial r} = 0 \quad [40]$$

$$\text{and at } r = 1,\ \frac{\partial c}{\partial r} = j_p \quad [41]$$

where c is the scaled concentration of the particle, r is the scaled radial variable in the spherical coordinate, and j_p is the scaled flux of the particle inside the electrode, which is a function of the applied current density.

The surface concentration (c_s) is given by:

$$c_s = c(r)|_{r=1} \quad [42]$$

In order to solve the model, a finite difference solution is used. The details of implementing finite difference solution (method of lines approach) can be found elsewhere,[24] and is not discussed here. The final set of equations obtained after implementing finite difference for N = 19 internal node points are given by:

$$\frac{dC_i}{dt} = \frac{C_{i+1} - 2C_i + C_{i-1}}{h^2} + \frac{2}{i\cdot h}\frac{C_{i+1} - C_{i-1}}{2\cdot h}, i = 1\ldots 19 \quad [43]$$

$$\frac{C_1 - C_0}{h} = 0 \quad [44]$$

Table II. Expression for the open circuit potential in the single particle model.

$$E_0 = \begin{cases} a_1 + a_2 C_s + a_3 {C_s}^2 + a_4 {C_s}^3 + \\ a_5 (C_s - a)^2 (\frac{1}{2} tanh(1000(C_s + 1)) + tanh(1000(C_s - a))) + \\ a_6 (C_s - b)^3 (1 - \frac{1}{2} tanh(1000(C_s + 1)) + tanh(1000(C_s - b))) + \\ a_7 (C_s - c)^3 (1 - \frac{1}{2} tanh(1000(C_s + 1)) + tanh(1000(C_s - c))) + \\ a_8 (C_s - d)^3 (1 - \frac{1}{2} tanh(1000(C_s + 1)) + tanh(1000(C_s - d))) + \\ a_9 (C_s - e)^3 (1 - \frac{1}{2} tanh(1000(C_s + 1)) + tanh(1000(C_s - e))); \end{cases}$$

$$\begin{aligned} a_1 &= 9.41894182550, \\ a_2 &= -20.8089294802, \\ a_3 &= 26.0321098756, \\ a_4 &= -11.2415464828, \\ a_5 &= -292.586540767, \\ a_6 &= -.212804379260 \\ a_7 &= 125.437252178, \\ a_8 &= -198.413506247, \\ a_9 &= 164.029238273 \\ a &= 0.96, b = 0.733, \\ c &= 0.575, d = 0.535, \\ e &= 0.466 \end{aligned}$$

$$\frac{C_{N+1} - C_N}{h} = j_p \quad [45]$$

$$C_s = c_s = C_{N+1} \quad [46]$$

$$h = \frac{1}{N+1} \quad [47]$$

where C_i is the concentration of the particle at the i^{th} node point in the radial direction. The manipulated variable for this case, is the dimensionless flux (j_p). The potential of the electrode (V) is defined according to a Nernst equation, as given by:

$$V(t) = E_0 - \frac{RT}{F} \log(C_s(t)) \quad [48]$$

where E_0 is the open-circuit potential of the electrode and is assumed to be a function of the surface concentration (C_s) of the electrode (as is the case in most battery models), R is the ideal gas constant. F is the Faraday's constant, and T is the temperature of the electrode, and is assumed to be 298 K. The expression for E_0 used as a function of the surface concentration is shown in Table II. The values of parameters are assumed only for theoretical purposes, and not versus any standard electrode. The initial conditions of all the variables are $C_i(0) = 0.5, V(0) = 4.09$ and $j_p(0) = 0$.

The measured variable is assumed to be V, and a set points of $V^{set} = [3.2V, 3.5V]$ are taken.

As in the previous case, the derivative of potential ($\frac{dV}{dt}$) is calculated by differentiating Equation 48. For this case,

$$\begin{matrix} Y = V \\ \frac{dV}{dt} = \frac{dE_0}{dC_s} \cdot \frac{dC_s}{dt} - \frac{RT}{F} \cdot \frac{1}{C_s} \cdot \frac{dC_s}{dt} \end{matrix} \quad [49]$$

Moreover, $\frac{\partial g}{\partial u}(y, z, u)$ (Equation 9) is not zero for this case.

The GMC formulation is written as follows:

$$\frac{dV}{dt} = K\left(V^{set} - V(t)\right) + \frac{K}{\tau_i} r(t) \quad [50]$$

$$\frac{dr}{dt} = \left(V^{set} - V(t)\right) \quad [51]$$

From Equations 49 and 50, we can get:

$$\frac{dE_0}{dC_s} \cdot \frac{dC_s}{dt} - \frac{RT}{F} \cdot \frac{1}{C_s} \cdot \frac{dC_s}{dt} = K\left(V^{set} - V(t)\right) + \frac{K}{\tau_i} r(t) \quad [52]$$

Equation 45 can be differentiated to get the derivative for $\frac{dC_s}{dt}$ (after substituting Equation 46) as

$$\frac{dC_s}{dt} = \frac{dC_{N+1}}{dt} = h \cdot \frac{dj_p}{dt} + \frac{dC_N}{dt} \quad [53]$$

From Equations 52 and 53, we get:

$$\begin{aligned} &\frac{dE_0}{dC_s} \cdot \left(h \cdot \frac{dj_p}{dt} + \frac{dC_N}{dt}\right) - \frac{RT}{F} \cdot \frac{1}{C_s} \cdot \left(h \cdot \frac{dj_p}{dt} + \frac{dC_N}{dt}\right) \\ &= K\left(V^{set} - V(t)\right) + \frac{K}{\tau_i} r(t) \end{aligned} \quad [54]$$

Equation 54 is solved along with Equations 43–48 to obtain the GMC control law. When there is no bound on the scaled flux, the equations to be solved are summarized as:

$$\left.\begin{aligned} &\frac{dC_i}{dt} = \frac{C_{i+1} - 2C_i + C_{i-1}}{h^2} + \frac{2}{i \cdot h} \frac{C_{i+1} - C_{i-1}}{2 \cdot h}, i = 1 \ldots 19 && \text{(a)} \\ &\frac{C_1 - C_0}{h} = 0 && \text{(b)} \\ &\frac{C_{N+1} - C_N}{h} = j_p && \text{(c)} \\ &C_s = c_s = C_{N+1} && \text{(d)} \\ &C_{avg}(t) = \frac{C_0(t) + 2\left(\sum_{i=1}^{N} C_i(t)\right) + C_{N+1}(t)}{2N+2} && \text{(e)} \\ &h = \frac{1}{N+1} && \text{(f)} \\ &V(t) = E_0 - \frac{RT}{F} \log(C_s(t)) && \text{(g)} \\ &\frac{dr}{dt} = \left(V^{set} - V(t)\right) && \text{(h)} \\ &\frac{dE_0}{dC_s} \cdot \left(h \cdot \frac{dj_p}{dt} + \frac{dC_N}{dt}\right) - \frac{RT}{F} \cdot \frac{1}{C_s} \cdot \left(h \cdot \frac{dj_p}{dt} + \frac{dC_N}{dt}\right) \\ &\quad = K\left(V^{set} - V(t)\right) + \frac{K}{\tau_i} r(t) && \text{(i)} \end{aligned}\right\} \quad [55]$$

The controller tuning parameter K is chosen as 1 and τ_i is assumed to be 1000. Figure 4a shows the profiles of potential with time for two different set points and the corresponding control profiles are shown in

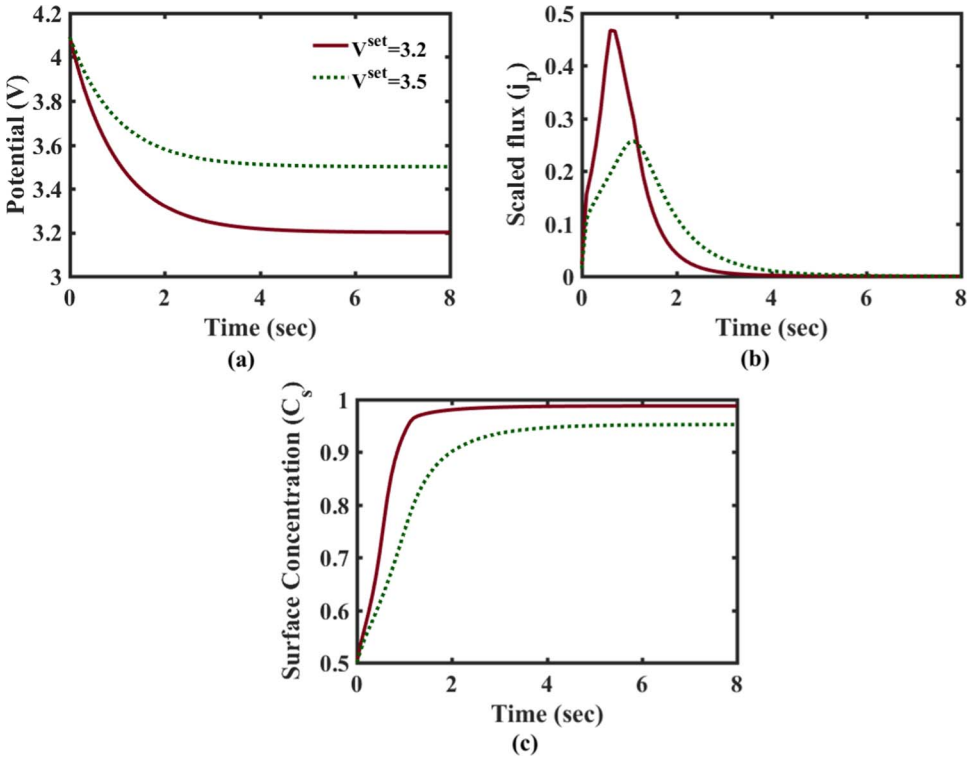

Figure 4. Profiles of (a) potential (b) scaled flux (j_p) and (c) surface concentration (C_s) with time for the single particle model.

Figure 4b. The profiles for surface concentration are shown in Figure 4c.

In order to implement bounds, same procedure as discussed for the unbounded case is followed, and the equations are again summarized below but with bounds on the manipulated variable j_p.

$$\left.\begin{aligned}
&\frac{dC_i}{dt} = \frac{C_{i+1} - 2C_i + C_{i-1}}{h^2} + \frac{2}{i \cdot h}\frac{C_{i+1} - C_{i-1}}{2 \cdot h}, i = 1 \ldots 19 && \text{(a)}\\
&\frac{C_1 - C_0}{h} = 0 && \text{(b)}\\
&\frac{C_{N+1} - C_N}{h} = j_p && \text{(c)}\\
&C_s = c_s = C_{N+1} && \text{(d)}\\
&h = \frac{1}{N+1} && \text{(e)}\\
&V(t) = E_0 - \frac{RT}{F}\log\left(C_s(t)\right) && \text{(f)}\\
&\frac{dr}{dt} = \left(V^{set} - V(t)\right) && \text{(g)}\\
&\frac{dE_0}{dC_s}\cdot\left(h\cdot\frac{dj_1}{dt} + \frac{dC_N}{dt}\right) - \frac{RT}{F}\cdot\frac{1}{C_s}\cdot\left(h\cdot\frac{dj_1}{dt} + \frac{dC_N}{dt}\right) && \text{(h)}\\
&= K\left(V^{set} - V(t)\right) + \frac{K}{\tau_i}r(t) && \text{(i)}\\
&j_p = \min\left(0.20, \max\left(0, j_1\right)\right) && \text{(j)}
\end{aligned}\right\} \quad [56]$$

Figure 5 shows the profiles obtained for an upper bound on j_p of 0.2 for different set points on voltage. The control profiles obtained in this case again drive the measured variable to its required set point.

Reformulated pseudo 2 dimensional (P2D) model.—Pseudo 2-Dimensional (P2D) model proposed by Doyle et al.[25] is one of the most popular physics-based lithium-ion battery model. Other approaches[26,27] have been proposed for efficient simulation of battery models. Northrop et al.[28,29] published a reformulated battery model, based on the original P2D model, and the reformulated model was used in this work to obtain the control profiles after implementing GMC. The set of equations and the corresponding parameters of the battery model are listed in Table III, Table IV and Table V (Reference 29).

We present two cases for this model, even though GMC formulation can be applied for more variables.

Set point for the charge stored in the battery.—In this case, the objective is to find the current profiles to obtain the final charge stored to reach a desired set point Q^{set}, with a bound on the applied current. Mathematically,

Find $I_{app}(t)$ subject to the model equations given in Table III, and the constraints

$$Q\left(t_f\right) = Q^{set} \quad [57]$$

$$0 \le I_{app}(t) \le 3C \quad [58]$$

where $I_{app}(t)$ is the applied current, $Q(t)$ is the charged stored in the battery, Q^{set} is the set-point for the charge, C is the capacity of the battery and t_f is the final time. The value of Q^{set} for this study is taken to be 14 A-hr.

For this problem (comparing with Equation 2),

$$Y = Q$$

The full derivative of the measured variable is directly available from the model thereby resulting in a direct equation for I_{app} instead of $\frac{dI_{app}}{dt}$. For this case, in Equation 9, $\frac{\partial g}{\partial u}(y, z, u)$ is not zero.

The equation for charge stored is given by:

$$\frac{dQ}{dt} = I_{app} \quad [59]$$

As in the previous examples, the GMC equation can be written as:

$$\frac{dQ}{dt} = K\left(Q^{set} - Q(t)\right) + \frac{K}{\tau_i}r(t) \quad [60]$$

Table III. Equations for P2D thermal model.

Governing Equation	Boundary Conditions
Positive Electrode	
$\varepsilon_p \frac{\partial c_p}{\partial t} = \frac{1}{l_p}\frac{\partial}{\partial X}[\frac{D_{\text{eff,p}}}{l_p}\frac{\partial c_p}{\partial X}] + a_p(1-t_+)j_p$	$\frac{\partial c_p}{\partial X}\|_{X=0} = 0$ $\frac{-D_{\text{eff,p}}}{l_p}\frac{\partial c_p}{\partial X}\|_{X=1} = \frac{-D_{\text{eff,s}}}{l_s}\frac{\partial c_s}{\partial X}\|_{X=0}$
$\frac{-\sigma_{\text{eff,p}}}{l_p}(\frac{\partial \Phi_{1,p}}{\partial X}) - \frac{\kappa_{\text{eff,p}}}{l_p}(\frac{\partial \Phi_{2,p}}{\partial X}) + \frac{2\kappa_{\text{eff,p}}RT}{F}\frac{(1-t_+)}{l_p}(\frac{\partial \ln c_p}{\partial X}) = I$	$\frac{\partial \Phi_{2,p}}{\partial X}\|_{X=0} = 0$ $\frac{-\kappa_{\text{eff,p}}}{l_p}\frac{\partial \Phi_{2,p}}{\partial X}\|_{X=1} = \frac{-\kappa_{\text{eff,s}}}{l_s}\frac{\partial \Phi_{2,s}}{\partial X}\|_{X=0}$
$\frac{1}{l_p}\frac{\partial}{\partial X}[\frac{\sigma_{\text{eff,p}}}{l_p}\frac{\partial}{\partial X}\Phi_{1,p}] = a_p F j_p$	$(\frac{1}{l_p}\frac{\partial \Phi_{1,p}}{\partial X})\|_{X=0} = -\frac{I}{\sigma_{eff,p}}$ $\frac{\partial \Phi_{1,p}}{\partial X}\|_{X=1} = 0$
$\frac{\partial c_p^s}{\partial t} = \frac{1}{r^2}\frac{\partial}{\partial r}[r^2 D_p^s \frac{\partial c_p^s}{\partial r}]$	$\frac{\partial c_p^s}{\partial r}\|_{r=0} = 0$ $-D_p^s \frac{\partial c_p^s}{\partial r}\|_{r=R_s} = j_p$
$\rho_p C_{p,p}\frac{dT_p}{dt} = \frac{1}{l_p}\frac{\partial}{\partial X}[\frac{\lambda_p}{l_p}\frac{\partial T_p}{\partial X}] + Q_{\text{rxn,p}} + Q_{\text{rev,p}} + Q_{\text{ohm,p}}$	$-Kef f_p \frac{\partial T_p}{\partial X}\|_{X=0} = h_{env}(T_p\|_{X=0} - T_{air})$ $-\frac{\lambda_p}{l_p}\frac{\partial T_p}{\partial X}\|_{X=1} = -\frac{\lambda_s}{l_s}\frac{\partial T_s}{\partial X}\|_{X=0}$
Separator	
$\varepsilon_s \frac{\partial c_s}{\partial t} = \frac{1}{l_s}\frac{\partial}{\partial X}[\frac{D_{\text{eff,s}}}{l_s}\frac{\partial c_s}{\partial X}]$	$c_p\|_{X=1} = c_s\|_{X=0}$ $c_s\|_{X=1} = c_n\|_{X=0}$
$-\frac{\kappa_{\text{eff,s}}}{l_s}(\frac{\partial \Phi_{2,s}}{\partial X}) + \frac{2\kappa_{\text{eff,s}}RT}{F}\frac{(1-t_+)}{l_s}(\frac{\partial \ln c_S}{\partial X}) = I$	$\Phi_{2,p}\|_{X=1} = \Phi_{2,s}\|_{X=0}$ $\Phi_{2,s}\|_{X=1} = \Phi_{2,n}\|_{X=0}$
$\rho_s C_{p,s}\frac{dT_s}{dt} = \frac{1}{l_s}\frac{\partial}{\partial X}[\frac{\lambda_s}{l_s}\frac{\partial T_s}{\partial X}] + Q_{\text{ohm,s}}$	$T_p\|_{X=1} = T_s\|_{X=0}$ $T_s\|_{X=0} = T_n\|_{X=1}$
Negative Electrode	
$\varepsilon_n \frac{\partial c_n}{\partial t} = \frac{1}{l_n}\frac{\partial}{\partial X}[\frac{D_{\text{eff,n}}}{l_n}\frac{\partial c_n}{\partial X}] + a_n(1-t_+)j_n$	$\frac{\partial c_n}{\partial X}\|_{X=1} = 0$ $\frac{-D_{\text{eff,s}}}{l_s}\frac{\partial c_s}{\partial X}\|_{X=1} = \frac{-D_{\text{eff,n}}}{l_n}\frac{\partial c_n}{\partial X}\|_{X=0}$
$\frac{-\sigma_{\text{eff,n}}}{l_n}(\frac{\partial \Phi_{1,n}}{\partial X}) - \frac{\kappa_{\text{eff,n}}}{l_n}(\frac{\partial \Phi_{2,n}}{\partial X}) + \frac{2\kappa_{\text{eff,n}}RT}{F}\frac{(1-t_+)}{l_n}(\frac{\partial \ln c_n}{\partial X}) = I$	$\Phi_{2,n}\|_{X=1} = 0$ $\frac{-\kappa_{\text{eff,s}}}{l_s}\frac{\partial \Phi_{2,s}}{\partial X}\|_{X=1} = \frac{-\kappa_{\text{eff,n}}}{l_n}\frac{\partial \Phi_{2,n}}{\partial X}\|_{X=0}$
$\frac{1}{l_n}\frac{\partial}{\partial X}[\frac{\sigma_{\text{eff,n}}}{l_n}\frac{\partial}{\partial X}\Phi_{1,n}] = a_n F(j_n + j_{sei})$	$\frac{\partial \Phi_{1,n}}{\partial X}\|_{X=0} = 0$ $(\frac{1}{l_n}\frac{\partial \Phi_{1,n}}{\partial X})\|_{X=1} = -\frac{I}{\sigma_{eff,n}}$
$\frac{\partial c_n^s}{\partial t} = \frac{1}{r^2}\frac{\partial}{\partial r}[r^2 D_n^s \frac{\partial c_n^s}{\partial r}]$	$\frac{\partial c_n^s}{\partial r}\|_{r=0} = 0$ $-D_n^s \frac{\partial c_n^s}{\partial r}\|_{r=R_s} = j_n$
$\rho_n C_{p,n}\frac{dT_n}{dt} = \frac{1}{l_n}\frac{\partial}{\partial X}[\frac{\lambda_n}{l_n}\frac{\partial T_n}{\partial X}] + Q_{\text{rxn,n}} + Q_{\text{rev,n}} + Q_{\text{ohm,n}}$	$-\frac{\lambda_s}{l_s}\frac{\partial T_s}{\partial X}\|_{X=1} = -\frac{\lambda_n}{l_n}\frac{\partial T_n}{\partial X}\|_{X=0}$ $-Kef f_n \frac{\partial T_n}{\partial X}\|_{X=1} = h_{env}(T_{air} - T_n\|_{X=1})$

$$\frac{dr}{dt} = Q^{set} - Q(t) \quad [61]$$

From Equations 59 and 60, the equation for applied current can be written as:

$$I_{app} = K\left(Q^{set} - Q(t)\right) + \frac{K}{\tau_i} r(t) \quad [62]$$

The bounds in Equation 58, are applied on the current as:

$$I_{app}(t) = \min\left(54, \max\left(0, K\left(Q^{set} - Q(t)\right) + \frac{K}{\tau_i} r(t)\right)\right) \quad [63]$$

where 54 A/m^2 is assumed to be the current equivalent for 3 C. The controller tuning parameter is chosen as K = 0.01, and $\tau_i = 1e-4$. Equation 63 can be used along with the model equations mentioned in Table III, to obtain the GMC control profile.

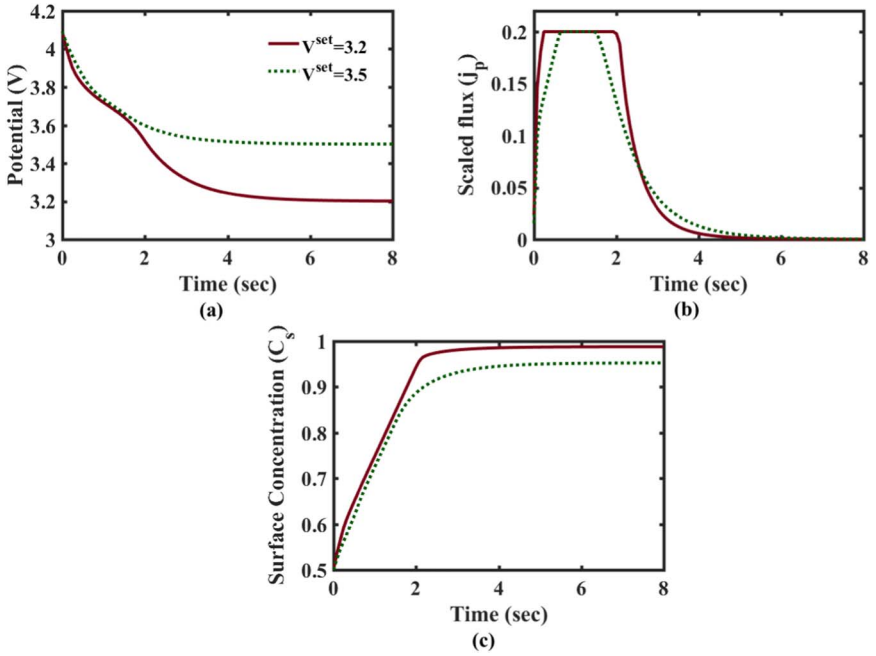

Figure 5. Profiles of (a) Potential, (b) Scaled flux (j_p) and (c) Surface concentration (C_s) with time for the single particle model.

Figure 6a, shows the profile of charge stored reaching the desired set-point and the corresponding applied current profile is shown in Figure 6b. Since for this case, there is no constraint given on temperature, or voltage, the battery is charged at a constant current of *3C* that is the maximum bound on the current, until the charge stored reaches the desired set-point Q^{set}. After t = 934 seconds, the current falls to zero in order to keep the charge stored at the desired set-point Q^{set}. Figures 6c and 6d show the corresponding changes in voltage and temperature of this constant current charging case, respectively. The temperature and voltage both increase steadily as expected until the current is non-zero. After t = 934 seconds, when the current becomes zero, the temperature starts to fall, whereas voltage remains constant at the open-circuit value.

Set point for voltage of the cell.—Consider a cell being charged from a fully discharged state. The set point for the voltage while charging is set to be $V^{set} = 4.2$ V. In the P2D model, the voltage of the cell (V) is given by the equation:

$$V(t) = \phi_1(t)|_{x=0} - \phi_1(t)|_{x=L_{pos}+L_{sep}+L_{neg}} \quad [64]$$

where $\phi_1(t)$ denotes the potential of the solid phase, and L_{pos}, L_{sep}, L_{neg}, represent the thicknesses of the positive electrode, separator and negative electrode of the cell, respectively.

This case is similar to the case presented in Thin film nickel hydroxide electrode section (c), where the explicit derivative for the measured variable (voltage) is not given by the model equations.

For this case,

$$Y = V(t)$$

and $\frac{\partial g}{\partial u}(y, z, u)$ (in Equation 9) is not zero.

Through substitution of other model equations, it can be shown that the potential of the cell is directly dependent on the applied current (I_{app}). Equation 64 is differentiated with time to get the derivative of potential. In order to find derivative for other terms occurring in

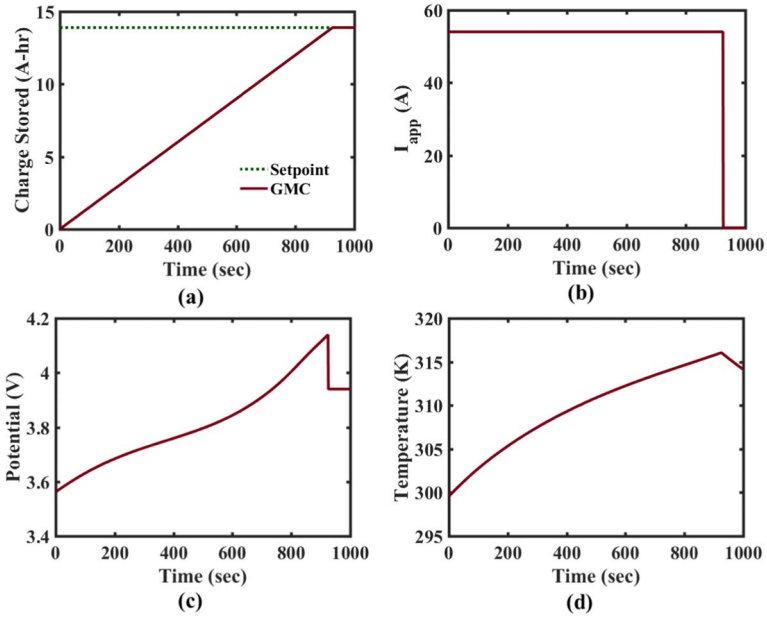

Figure 6. Profiles of (a) Charge stored, (b) Applied current, (c) Potential and (d) Temperature with time for the reformulated P2D model.

Table IV. Additional Equations.[29]

$$Q_{\text{rxn},i} = Fa_i j_i(\Phi_{1,i} - \Phi_{2,i} - U_i),\ i = p, n$$

$$Q_{\text{rev},i} = Fa_i j_i T_i \frac{\partial U_i}{\partial T},\ i = p, n$$

$$Q_{\text{ohm},i} = \sigma_{\text{eff},i}(\frac{1}{l_i}\frac{\partial \Phi_{1,i}}{\partial X})^2 + \kappa_{\text{eff},i}(\frac{1}{l_i}\frac{\partial \Phi_{2,i}}{\partial X})^2 + \frac{2\kappa_{\text{eff},i}RT_i}{F}(1 - t_+^0)\frac{1}{l_i^2}\frac{1}{c_i}\frac{\partial c_i}{\partial X}\frac{\partial \Phi_{2,i}}{\partial X},\ i = p, n$$

$$Q_{\text{ohm,s}} = \kappa_{\text{eff},s}(\frac{1}{l_s}\frac{\partial \Phi_{2,s}}{\partial x})^2 + \frac{2\kappa_{\text{eff},s}RT_s}{F}(1 - t_+^0)\frac{1}{c_s}\frac{1}{l_s^2}\frac{\partial c_s}{\partial X}\frac{\partial \Phi_{2,i}}{\partial X}$$

$$U_i(T_i, \theta_i) = U_{\text{i,ref}}(T_{\text{ref}}, \theta_i) + (T_i - T_{\text{ref}})[\frac{dU_i}{dT}]|_{T_{\text{ref}}},\ i = p, n$$

$$D^s_{i,eff} = D^s_i \exp(-\frac{E_a^{D_i^s}}{R}[\frac{1}{T} - \frac{1}{T_{ref}}]), i = p, n$$

$$k_{i,eff} = k_i \exp(-\frac{E_a^{k_i}}{R}[\frac{1}{T} - \frac{1}{T_{ref}}]), i = p, n$$

Equation 64, all the algebraic equations are differentiated with time, to convert the system of differential algebraic equations (DAEs) to a system of ordinary differential equations (ODEs). GMC formulation is then applied for this case as:

$$\frac{dV}{dt} = K\,(4.2 - V\,(t)) + \frac{K}{\tau_i} r\,(t) \quad [65]$$

$$\frac{dr}{dt} = 4.2 - V(t) \quad [66]$$

The $\frac{dV}{dt}$ term appearing in the differentiation of all the algebraic equations, is eliminated by substituting Equation 65. The math followed is similar to the set point for potential explained for potential explained in the thin film nickel hydroxide section (c). The tuning parameter K is assumed to be 0.01 and τ_i is taken to be 100. Figure 7 (solid red curve) shows the results when no bound is imposed on the applied current and the potential for the PI case. In this case, the voltage of the battery goes above 4.2 V, ultimately driving the voltage to its desired set point. However, for these sets of tuning parameters, the battery is overcharged before set-point for voltage is reached, which causes an increase in the rate of battery degradation. Figure 7 also shows the effect of increasing the τ_i value to 1e9 (dashed green curve), which drives the voltage to its set-point without going above the set-point. However, it should be noted that increasing the τ_i value decreases the impact of the integral term.

Hence, for this case, GMC formulation is applied using only a proportional term (P-Controller), as:

$$\frac{dV}{dt} = K\,(4.2 - V\,(t)) \quad [67]$$

For this case, the voltage of the battery reaches its set point of 4.2 V, whereas the current increases first until 189 s, and decreases thereafter, as shown in Figure 8.

Set point for voltage with bounds on applied current.—In the next case, the set point of 4.2 V is applied to the potential as in case (b), but additional bounds are added for applied current as shown below.

$$0 \le I_{app}\,(t) \le 30A/m^2 \quad [68]$$

This case is similar to the single particle model case described above. Figure 9a shows the change in voltage vs time for this case, and Figure 9b shows the GMC control profile for current.

Through these examples, it can be seen that the voltage reaches its desired set point for both, the bounded as well as the unbounded current case. The bounded case is closer to the real life scenario, where an upper limit is usually applied on the charging current. The advantage of implementing control through GMC is that the variables are only to be integrated in time. We implemented the control scheme using the direct iteration-free DAE numerical solvers previously reported by Lawder et al.[30] This makes the approach more robust and fail-proof, as standard optimizers fail to find the optimal solution often times because of their inability to find consistent initial conditions for algebraic variables. It should be noted that for simple first order or second order processes, the time constants of the processes can be related to the tuning of the GMC parameters. However, physics-based battery models have multiple dynamics, and we choose an approach to modify the tuning parameters until no effect is seen in the profiles of control and measured variables. The arbitrariness in the tuning parameters is an inherent limitation of the GMC approach.

Performance of GMC under Model Uncertainty

Lee and Sullivan[14] have discussed the impact of uncertainty in parameters in their original manuscript. In this section, we summarize the same and discuss the uncertainty for the thin-film electrode model.

Table V. List of parameters for the P2D model.[29]

Symbol	Parameter	Positive Electrode	Separator	Negative Electrode	Units
σ_i	Solid phase conductivity	100		100	S/m
$\varepsilon_{f,i}$	Filler fraction	0.025		0.0326	
ε_i	Porosity	0.385	0.724	0.485	
Brugg	Bruggman Coefficient		4		
D	Electrolyte diffusivity	7.5×10^{-10}	7.5×10^{-10}	7.5×10^{-10}	m^2/s
D_i^s	Solid Phase Diffusivity	1.0×10^{-14}		3.9×10^{-14}	m^2/s
k_i	Reaction Rate constant	2.334×10^{-11}		5.031×10^{-11}	$mol/(s\ m^2)/(mol/m^3)^{1+\alpha a,i}$
$c^s_{i,\max}$	Maximum solid phase concentration	51554		30555	mol/m^3
$c^s_{i,0}$	Initial solid phase concentration	25751		26128	mol/m^3
c_0	Initial electrolyte concentration		1000		mol/m^3
$R_{p,i}$	Particle Radius	2.0×10^{-6}		2.0×10^{-6}	M
a_i	Particle Surface Area to Volume	885000		723600	m^2/m^3
l_i	Region thickness	80×10^{-6}	25×10^{-6}	88×10^{-6}	M
t_+	Transference number		0.364		
F	Faraday's Constant		96487		C/mol
R	Gas Constant		8.314		J/(mol K)
T_{ref}	Temperature		298.15		K
P	Density	2500	1100	2500	kg/m^3
C_p	Specific Heat	700	700	700	J/(kg K)
Λ	Thermal Conductivity	2.1	0.16	1.7	J/(m K)
$E_a^{D_i^s}$	Activation Energy for Temperature Dependent Solid Phase Diffusion	5000		5000	J/mol
$E_a^{k_i}$	Activation Energy for Temperature Dependent Reaction Constant	5000		5000	J/mol

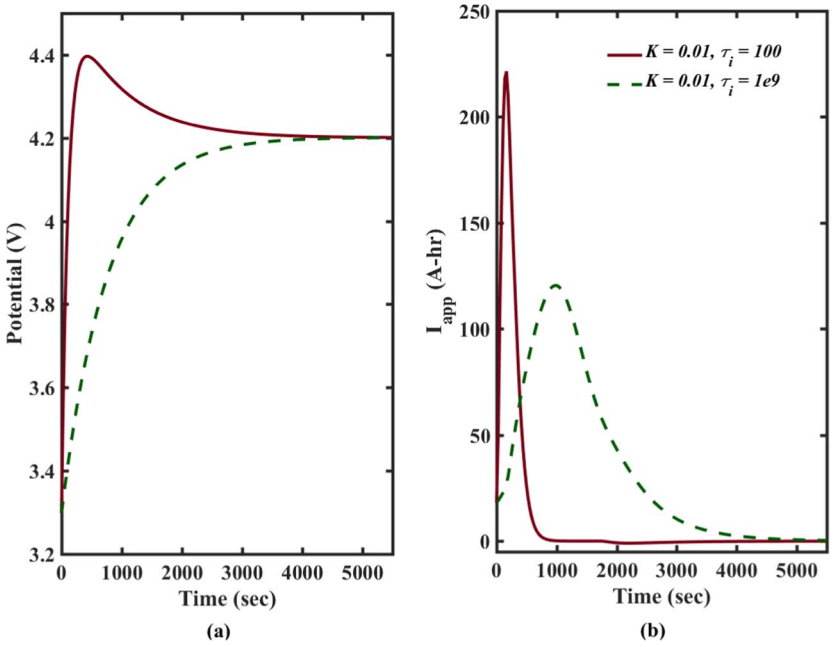

Figure 7. Profiles of (a) Potential (b) Applied current vs time for the P2D model obtained using PI controller.

Consider the plant model given by Equations 7 and 8 and the process model containing uncertainty given by:

$$\frac{dy}{dt} = \widehat{f}\,(y, z, u) \qquad [69]$$

$$\widehat{g}\,(y, z, u) = 0 \qquad [70]$$

The GMC formulation for the process model, where set point is given for the algebraic variable is written as:

$$\frac{d\widehat{g}}{dt} = \frac{\partial \widehat{g}}{\partial y}(y, z, u) \cdot f\,(y, z, u) + \frac{\partial \widehat{g}}{\partial y}(y, z, u) \cdot \left[K\left(z^{set} - z\right) + \frac{K}{\tau_i}\int_0^t \left(z^{set} - z\right) d\tau\right] + \frac{\partial \widehat{g}}{\partial u}(y, z, u) \cdot \frac{du}{dt} = 0 \qquad [71]$$

To solve GMC under model uncertainty, Equation 71 is used to obtain the control profile and solved along with Equations 7 and 8. For the thin-film electrode model, the model uncertainty is considered by perturbing the parameters $i_{0,1}$, ϕ_{01}, T, W by $\pm 10\%$. Potential (algebraic variable) is chosen to reach its desired set-point ϕ_1^{set} in the presence of uncertain parameters mentioned above. The potential profiles obtained are shown in Figure 10 and it can be observed that the GMC approach gives robust performance under model uncertainty, as the controlled variable reaches its desired set-point in every case.

Conclusions

Generic model control is applied for different types of battery models such as thin film nickel hydroxide electrode, single particle model, along with a reformulated pseudo 2D model. The conventional GMC approach is extended for DAEs as well as for problems

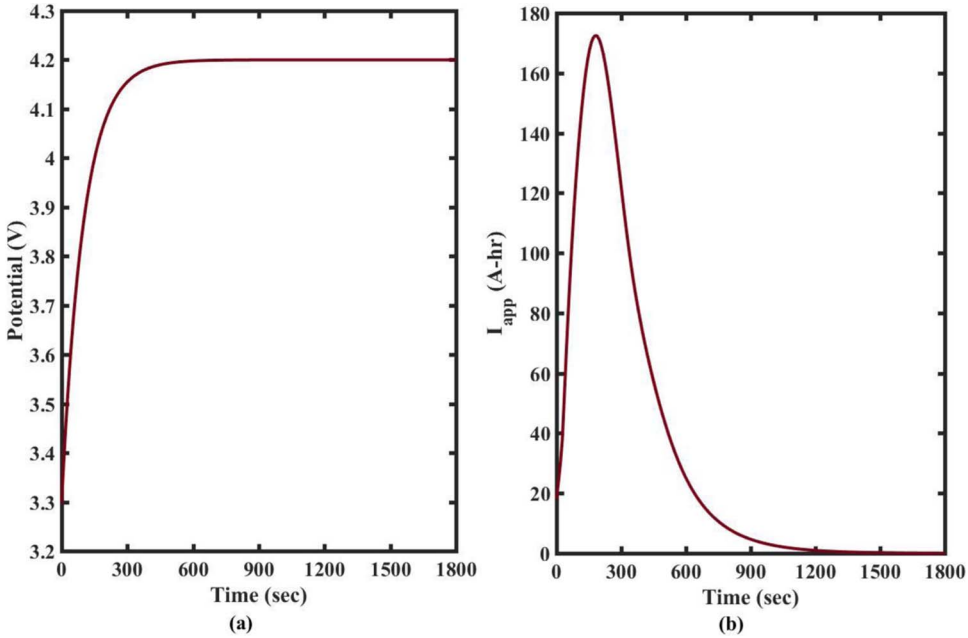

Figure 8. Profiles of (a) Potential (b) Applied current density vs time for the reformulated P2D model using P-controller.

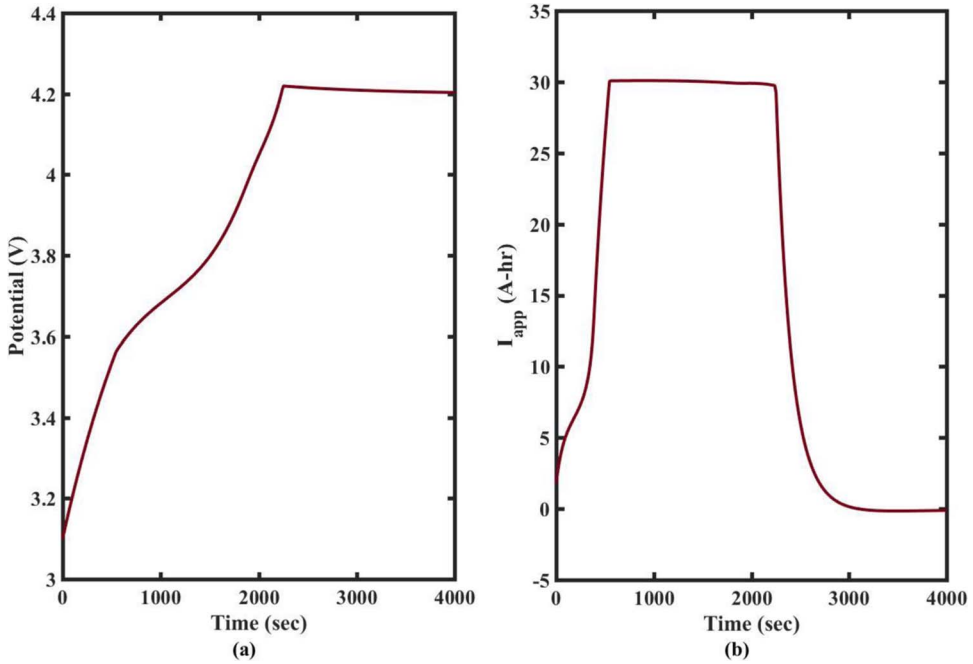

Figure 9. Profiles of (a) Potential (b) Applied current density vs time for the reformulated P2D model using P-Controller.

involving the direct correlation between the measured and the manipulated variable. The results are presented for various case studies, and the measured variable is shown to reach the desired set point in all cases. The approach is found to be extremely robust and fail-safe. Future work involves the implementation of the GMC control scheme for problems involving constraints on various state variables (for example, bounds on voltage and temperature for the P2D model). In the GMC framework, problems involving constraints or bounds has to be solved as an optimization problem. The constraint handling strategy and the need for performing optimization in the GMC framework will be explored in a future publication. The method will also be extended to explore the control profiles for single input multiple objective case, like minimizing the capacity fade while maximizing the charge stored in the battery, while maintaining the temperature and voltage constraints, and for process and plant models with time delays.

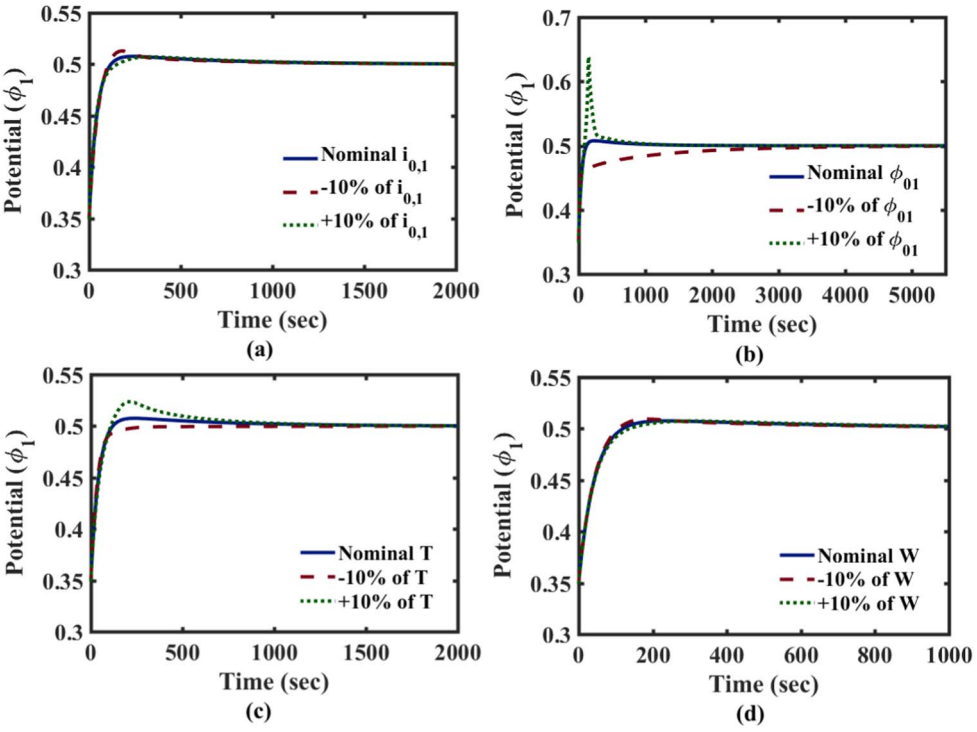

Figure 10. Profiles of potential reaching its sepecificed set-point, where parameters (a) Exchange current density, (b) Equilibrium potential, (c) Temperature and (d) Mass of the active material are perturbed by $\pm 10\%$.

Acknowledgments

The authors thank the Department of Energy (DOE) for providing partial financial support for this work, through the Advanced Research Projects Agency (ARPA-E) award number DE-AR0000275. The authors would also like to thank the Clean Energy Institute (CEI) at the University of Washington (UW) and the Washington Research Foundation (WRF) for their monetary support for this work.

List of Symbols

c	Electrolyte concentration
c^s	Solid Phase Concentration
D	Liquid phase Diffusion coefficient
D_{eff}	Effective Diffusion coefficient
D^s	Solid phase diffusion coefficient
E_a	Activation Energy
F	Faraday's Constant
$Iapp$	Applied Current
j	Pore wall flux
K	Proportional Gain
k	Reaction rate constant
l	Length of region
R	Particle Radius, or Residual
t_+	Transference number
T	Temperature
U	Open Circuit Potential
W	Mass of the active material

Greek

ε	Porosity
ε_f	Filling fraction
θ	State of Charge
κ	Liquid phase conductivity
σ	Solid Phase Conductivity
Φ_1	Solid Phase Potential
Φ_2	Liquid Phase Potential
τ_i	Integral Time Constant

Subscripts

eff	Effective, as for diffusivity or conductivity
c	Related to Electrolyte concentration
c^s	Related to Solid Phase concentration
n	Related to the negative electrode—the anode
p	Related to the positive electrode—the cathode
s	Related to the separator
Φ_1	Related to the solid phase potential
Φ_2	Related to the liquid phase potential

Superscripts

avg	Average, as for solid phase concentration
$surf$	Surface, as for solid phase concentration
s	Related to Solid Phase

References

1. S. Santhanagopalan and R. E. White, *Journal of Power Sources*, **161**, 1346 (2006).
2. S. J. Moura, N. A. Chaturvedi, and M. Krstic in *Proceedings of the American Control Conference*, p. 559 (2012).
3. B. Suthar, V. Ramadesigan, P. W. C. Northrop, B. Gopaluni, S. Santhanagopalan, R. D. Braatz, and V. R. Subramanian, in *American Control Conference (ACC)*, p. 5350, Seattle, WA, USA (2013).
4. D. D. Domenica, G. Fiengo, and A. Stefanopoulou, in *Proceedings of the IEEE Conference on Control Applications*, p. 702 (2008).
5. D. D. Domenica, A. Stefanopoulou, and G. Fiengo, *Journal of Dynamic Systems, Measurement and Control* **132**, 061302 (2010).
6. C. R. Cutler, *Dynamic Matrix Control: An Optimal Multivariable Control Algorithm with Consraints*, University of Houston, Houston, Texas, (1983).
7. C. E. Garcia and M. Morari, *Industrial & Engineering Chemistry Process Design and Development*, **21**, 308 (1982).
8. J. Richalet, A. Rault, J. L. Testud, and J. Papon, *Automatica*, **14**, 413 (1978).
9. R. N. Methekar, V. Ramadesigan, R. D. Braatz, and V. R. Subramanian, *ECS Transactions*, **25**, 139 (2010).
10. S. K. Rahimian, S. C. Rayman, and R. E. White, *Journal of the Electrochemical Society*, **157**, A1302 (2010).
11. H. E. Perez, X. Hu, and S. J. Moura, in *American Control Conference (ACC)*, p. 4000, Boston (2016).
12. B. Suthar, P. W. C. Northrop, R. D. Braatz, and and V. R. Subramanian, *Journal of the Electrochemical Society*, **161**, F3144 (2014).
13. A. Hoke, A. Brissette, K. Smith, A. Pratt, and D. Maksimovic, *IEEE Journal of Emerging and Selected Topics in Power Electronics*, **2**, 691 (2014).
14. P. L. Lee and G. R. Sullivan, *Computers and Chemical Engineering*, **12**, 573 (1987).
15. R. D. Bartusiak, C. Georgakis, and M. J. Reilly, *Chem Eng Sci*, **44**, 1837 (1989).
16. S. M. Alsadaie and I. M. Mujtaba, *Journal of Process Control*, **44**, 92 (2016).
17. M. Barolo, G. B. Guarise, S. Rienzi, and A. Trotta, *Computers and Chemical Engineering*, **17**, S349 (1993).
18. S. Banerjee and A. K. Jana, *Journal of Process Control*, **24**, 235 (2014).
19. L. Cong, X. Liu, Y. Zhou, and Y. Sun, *AIChE*, **59**, 4133 (2013).
20. T. T. Leea, F. Y. Wanga, A. Islamb, and R. B. Newella, *Journal of Process Control*, **9**, 505 (1999).
21. A. S. A. El-Hamid, *World Applied Sciences Journal*, **18**, 1689 (2012).
22. J. B. Rawlings, *IEEE Control Systems*, **20**, 38 (2000).
23. B. Wu and R. E. White, *Computers and Chemical Engineering*, **25**, 301 (2001).
24. W. E. Schiesser, *The Numerical Method of Lines*, Academic Press (1991).
25. M. Doyle, T. F. Fuller, and J. Newman, *Journal of the Electrochemical Society*, **140**, 1526 (1993).
26. L. Cai and R. E. White, *Journal of Power Sources*, **217**, 248 (2012).
27. A. Bizeray, S. Zhao, S. R. Duncan, and D. A. Howey, *Journal of Power Sources*, **296**, 400 (2015).
28. P. W. C. Northrop, V. Ramadesigan, S. De, and V. R. Subramanian, *Journal of the Electrochemical Society*, **158**, A1461 (2011).
29. P. W. C. Northrop, M. Pathak, D. Rife, S. De, S. Santhanagopalan, and V. R. Subramanian, *Journal of the Electrochemical Society*, **162**, A940 (2016).
30. M. T. Lawder, V. Ramadesigan, B. Suthar, and V. R. Subramanian, *Computers and Chemical Engineering*, **82**, 283 (2015).